Colloid Polym Sci 276:709–714 (1998)
© Steinkopff Verlag 1998

ORIGINAL CONTRIBUTION

Y.-J. Park
M.C. Khew
C.C. Ho
J.-H. Kim

Kinetics of latex formation of PBMA latex in the presence of alkali soluble resin using atomic force microscopy

Received: 30 October 1997
Accepted: 20 March 1998

Y.-J. Park · J.-H. Kim (✉)
Department of Chemical Engineering
Yonsei University
134 Shinchon-dong Sudaemoon-Ku
120-749 Seoul
Korea
E-mail: polylab1@bubble.yonsei.ac.kr

M.C. Khew · C.C. Ho
Department of Chemistry
University of Malaya

Abstract The effect of alkali-soluble resin (ASR), poly(ethylene-co-acrylic acid), EAA, postadded to emulsifier-free monodisperse poly(butyl methacrylate) (PBMA) latexes on the kinetics of film formation was investigated using atomic force microscopy (AFM). Corrugation height of latex particles in films was monitored at various annealing temperatures as a function of annealing time. Enhanced polymer diffusion was found in a latex film containing ASR regardless of annealing temperature. With increasing annealing temperature, a much higher rate of polymer diffusion was found in latex films containing ASR. These results can be interpreted that the low molecular weight and low Tg EAA resin adsorbed at the particle surface is more susceptible to diffusion than that of the PBMA in the film formation stage, thus it enhances the mobility of PBMA polymer.

Key words Alkali soluble resin – poly(butyl methacrylate) – latex film formation – atomic force microscopy (AFM)

Introduction

Emulsion polymer latex is an important industrial product used in coatings, adhesives and thermoplastics. Film formation process from emulsion polymer latexes has been the subject of much attention both theoretically and experimentally [1–3]. It can be regarded as a three-stage process: (a) particle packing—increasing concentration of the latex and the formation of a dense packing of the latex particles; (b) particle deformation—deformation of the latex particles into polyeders and the beginning of coalescence by interfacial and capillary forces; and (c) particle coalescence—further coalescence by the interdiffusion of polymer chains of adjacent particles. This film formation process has been studied by non-radio fluorescence energy transfer, attenuated total reflectance FT-IR, small angle neutron scattering (SANS), freeze fracture and atomic force microscopes (AFM) [4–6].

The film formation process depends on latex characteristics (nature of polymer, particle size and distribution, particle morphology, nature and amount of surfactants, etc.) and experimental conditions (annealing temperature, evaporation rate of water, etc.). Little is known, however, about the role of alkali soluble resin (ASR) on latex film formation. It is well known that the amphiphilic polymers that consist of both hydrophobic and hydrophilic groups can stabilize polymer particles as the intermolecular and/or intramolecular hydrophobic interaction [7–9]. Several patents have claimed the use of durable emulsion polymers prepared using these types of copolymers, which has been applied to a variety of substrates such as floor tiles, countertops, wall and shower tiles and so forth [10–11].

In this paper, we studied the effect of ASR postadded to emulsifier-free monodisperse poly(butyl methacrylate) (PBMA) latexes on the kinetics of film formation using atomic force microscopy (AFM).

Experimental

Materials

Distilled water was used throughout. Butyl methacrylate (BMA) was purchased from Junsei Chemical Co. (Japan). It was purified by vacuum distillation and stored in a refrigerator. The initiator was potassium persulfate (KPS: Samchun Pure Chemical Ind., Ltd., Korea). The EAA, poly(ethylene-co-acrylic acid) [M_n: 19 000, M_w: 111 000, acid number: 120, $T_g = 5\,^{\circ}$C], obtained from Dow Chemical (USA) was used as received. The other chemicals used were of reagent grade.

Preparation and characterization of PBMA latexes

The latexes were prepared by emulsifier-free emulsion polymerization using the following formulation: 720 g of distilled water, 80 g of BMA, 0.8 g of KPS and 0.25 g of sodium bicarbonate were placed into a double-wall jacketed glass reactor equipped with a stirrer, a thermometer, a condenser, and a nitrogen gas inlet, then polymerized at 70 °C for 24 h and contain linear PBMA, $M_w = 4.4 \times 10^5$, $M_w/M_n = 3.2$. The particle mean diameter and size distribution were determined by the particle size analyzer (Capillary Hydrodynamic Fractionation, CHDF-1100, Matec Applied Sciences) and was found to be 370 nm and 1.004, respectively. All latex samples were purified by

Fig. 1 Images of the PBMA latex film with different annealing time: (A) 20 min, (B) 4 h, (C) 14 h and (D) 74 h

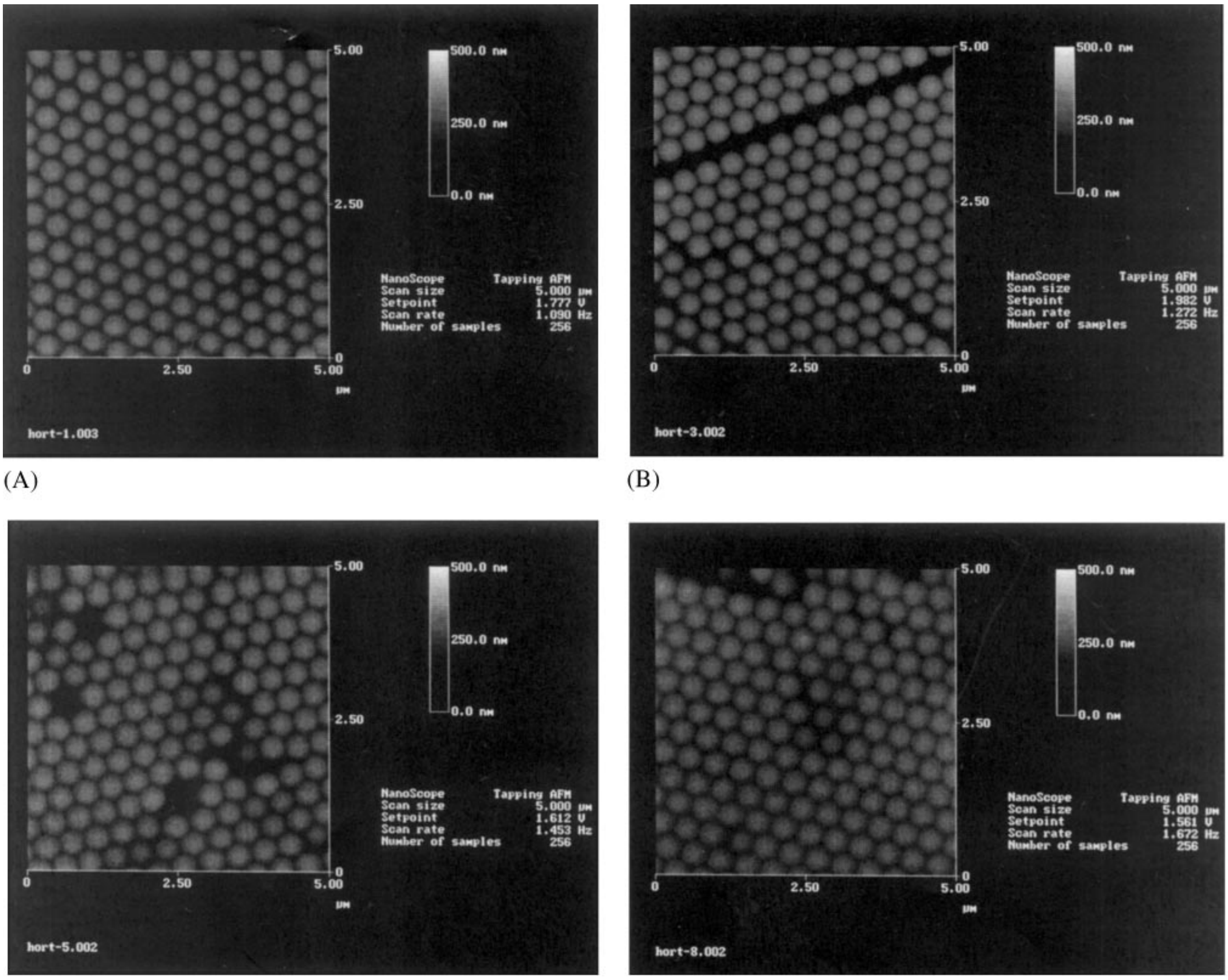

(A) (B) (C) (D)

the ion-exchange and serum replacement technique until the conductivity was less than 10^{-5} ohm^{-1}cm^{-1}.

Formation of latex films

Films were prepared by pouring a few drops of the mixture of PBMA latex and resin solution onto a freshly cleaved mica surface (cut into squares of ca. 10 mm × 10 mm) and allowing the film to dry slowly at room temperature in a desiccator. The effects of aging at elevated temperatures were investigated by annealing in a convection oven, at temperatures of either 25 °C, 60 °C, 70 °C or 90 °C for various lengths of time. After annealing, the samples were returned to a desiccator, in readiness for imaging by AFM.

Atomic force microscope imaging

All films were imaged with a Nanoscope III from Digital Instruments, Inc. The images were recorded with the piezoelectric scanner that has a lateral scan area of up to $12 \times 12\ \mu m^2$. The image was recorded in the Tapping mode, under ambient conditions.

Results and discussion

A study of latex film formation requires well-defined model latexes and reliable experimental instrumentation and procedures. The AFM is uniquely suited to follow the film formation process since it allows quantitative data to be obtained on the deformation of particles as film

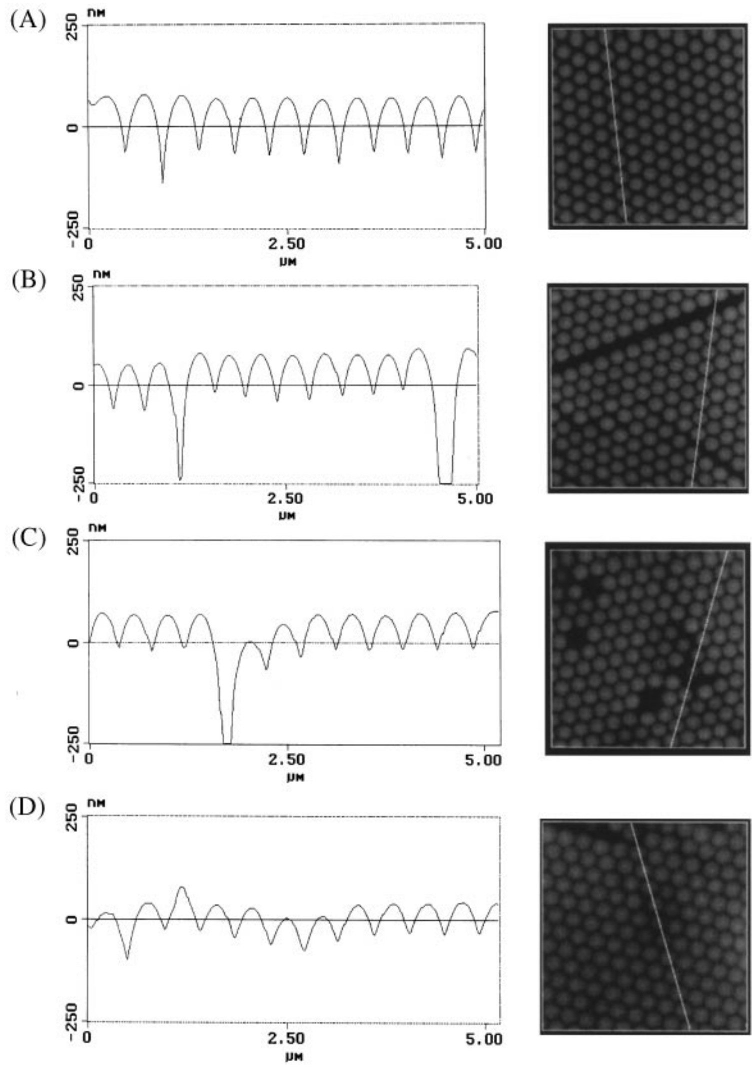

Fig. 2 Tracing of the z-axis profiles of the PBMA latex film with different annealing time: (A) 20 min, (B) 4 h, (C) 14 h and (D) 74 h

formation proceeds. This instrument can directly measure peak-to-valley dimensions ("corrugation heights") of the surface [12].

Figure 1 shows the typical surface images of latex film prepared from PBMA latex dispersion onto a mica surface, follow by drying in air at 25 °C. The surface structure of PBMA films has a high degree of order, consisting of face-centered cubic (FCC) packing in a highly ordered structure. As the annealing time increased, the individual particle contours became less well defined, and the film became flatter on a spherical scale of the particle diameter as shown in Fig. 2.

The peak-to-valley distance ΔZ can be measured to analyze diffusion of the polymer quantitatively from the cross section of the particle during deformation as shown in Fig. 3. Geometric considerations give the effective particle radius, r_{eff} as

$$r_{\text{eff}} = (\tfrac{1}{2})(R^2/\Delta Z + \Delta Z)\,, \tag{1}$$

$$r_{\text{eff}} = (6Dt)^{1/2}\,, \tag{2}$$

where, R is the average radius of the particles.

For Brownian diffusion, this effective radius will increase with time as $(6Dt)^{1/2}$, where D is the diffusion constant of the individual polymer. From the plot of r^2_{eff} vs. time, D value can be obtained using Eq. (2). It is the diffusion near the surface, which could be faster than in the bulk due to less hindrance to motion, as well as an extra driving force from the surface energy [13].

The latex films were annealed to investigate the time scale for polymer motion that occurs at the film surface during the annealing process. Figures 4 and 5 show the plots of corrugation heights and r^2_{eff} vs. time of the PBMA latex and PBMA latex containing 10 wt% EAA at temperatures of 25 °C, 60 °C, 70 °C or 90 °C for various lengths of time [14]. The slope of the fitted line gives the value for D. Figure 6 shows the plot of D as a function of temperature and D values are summarized in Table 1. The diffusion constant from energy transfer measurements (DET) for PBMA (M_n: 2.2–2.4 $\times 10^5$, M_w: 2.6–2.9 $\times 10^5$) at 90 °C is 0.6–2.9 $\times 10^{-15}$ cm^2 s^{-1} depending on diffusion time and DET models [15–17] and D for PBMA (M_w: 3 $\times$ 10^5) from SANS is 2.2–2.3 $\times 10^{-15}$ cm^2 s^{-1} [18]. These values are much slower than that of PBMA in this work from AFM measurements. This discrepancy is due to different measurement methods, which means that the D value from AFM measurements is for the initial stage of film formation and that of DET or SAN is for molecular motion of fully developed films.

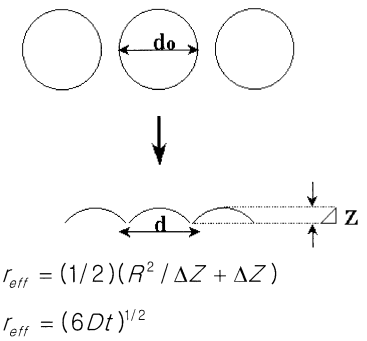

Fig. 3 Schematic diagram of the cross section of a particle cap during film formation, defining the interparticle spacing d and the peak-to-peak valley distance ΔZ

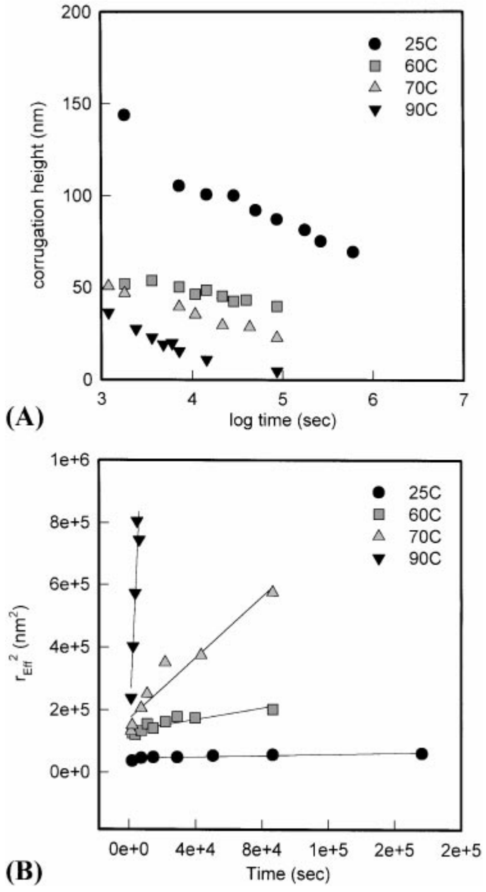

Fig. 4 Plots of (A) corrugation height and (B) effective particle radius vs. annealing time of PBMA latex film at 25 °C, 60 °C, 70 °C and 90 °C

Recently, Winnik et al. reported kinetic studies of polymer diffusion in latex films prepared from PBMA latex particles containing different amounts of acid groups at the particle surface. They showed that the polar component serves to slow down film formation and interdiffusion [9]. In the case of polymer film prepared using acid comonomer, a separate phase of polar material acts as an interconnecting phase in the newly formed film [19].

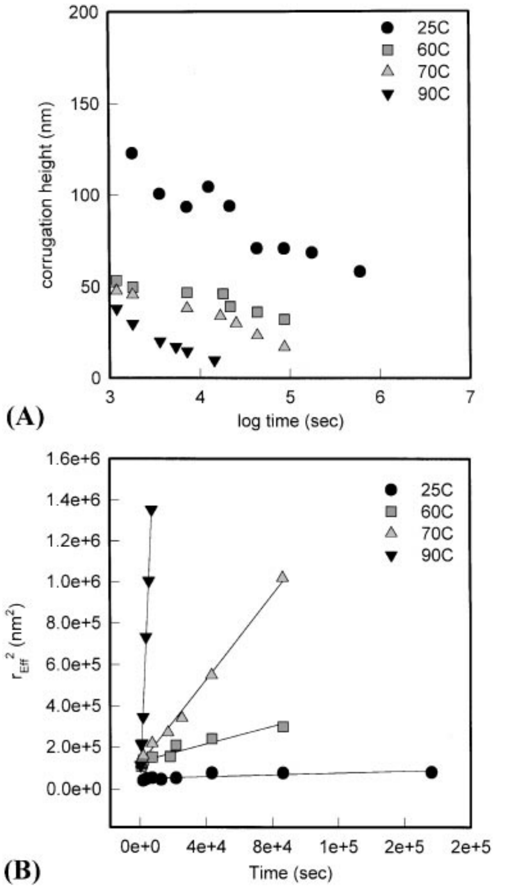

Fig. 5 Plots of (A) corrugation height and (B) effective particle radius vs. annealing time of PBMA latex film containing 10 wt% EAA at 25 °C, 60 °C, 70 °C and 90 °C

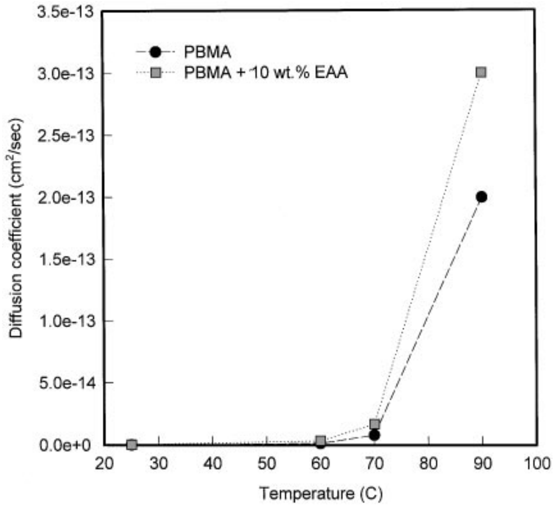

Fig. 6 Plot of diffusion coefficient vs. annealing time for latex films

Table 1 D (cm^2 s^{-1}) values for PBMA latex and PBMA latex containing 10% EAA

	25 °C	60 °C	70 °C	90 °C
PBMA	2.0e-16	1.5e-15	8.1e-15	2.e-13
PBMA + 10%EAA	3.7e-16	3.5e-15	1.7e-14	3.e-13
(PBMA + 10%EAA)/ (PBMA)	1.85	2.33	2.1	1.5

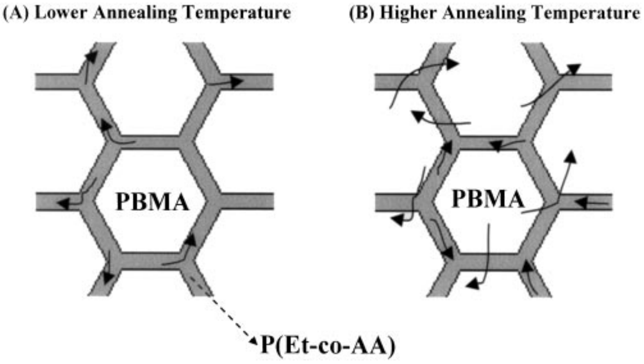

Fig. 7 Schematic diagram of film formation of PBMA latexes in the presence of EAA resin

However, *D* values for PBMA latex films, containing EAA are higher than that of PBMA latex films.

From the results presented above and based on the early works on the film formation, the kinetics of film formation in the presence of ASR can be drawn schematically in Fig. 7.

At lower annealing temperature than T_g of PBMA, low molecular weight and low T_g ASR adsorbed onto the particle surface diffuses first, and then PBMA polymer diffuses later. Also, cellular films with hydrophilic EAA walls separating hydrophobic PBMA materials are quite susceptible to the penetration of water [20], indicating that the so-called hydroplasticization effect could have occurred [21]. Therefore, the role of EAA in the diffusion would be to increase the mobility of PBMA polymers and to enhance their passing through the polar walls. This effect is profound at 60 °C and 70 °C. There is, however, little difference between a PBMA film and a PBMA film containing EAA in *D* value as shown in Table 1 at a much higher annealing temperature. This indicated that ASR adsorbed onto the particle surface and PBMA polymer diffuses almost simultaneously.

Conclusions

Atomic force microscopy was used to analyze the kinetics of film formation of PBMA latex containing ASR.

Enhanced polymer diffusion was found in a latex film containing ASR regardless of annealing temperature. With increasing annealing temperature, much higher rate of polymer diffusion was found in latex films containing ASR. The possible explanation of these observation is that, as the annealing proceeds, low molecular weight and low T_g EAA resin adsorbed at the particle surface is more susceptible to diffusion than that of the PBMA.

Acknowledgements The authors wish to acknowledge the financial support of the Korea Research Foundation made in the program year 1996 and the Korea Science and Engineering Foundation (KOSEF), project number 94-10-00-05-3.

References

1. Kim JD, Sperling LH, Klein A (1994) Macromolecules 27:6841
2. Yoo JY, Sperling LH, Glinka CJ, Klein A (1991) Macromolecules 24:2868
3. Juhue D, Lang J (1994) Macromolecules 27:695
4. Hahn K, Ley G, Schuller H, Oberthur R (1986) Colloid Polym Sci 264:1092
5. Wang YK, Kats A, Juhue D, Winnik MA (1992) Langmuir 8:1435
6. Hahn K (1985) Makromol Chem Suppl 10/11:447
7. Juhue D, Lang J (1993) Langmuir 9:792
8. Lee DY, Kim JH (1998) J Appl Polym Sci 69:543
9. Kim H-B, Winnik MA (1995) Macromolecules 28:2033
10. US patent (1993) 5 234 974
11. US patent (1979) 4 151 143
12. Lin F, Meier DJ (1995) Langmuir 11:2726
13. Goh MC, Juhue D, Wang Y, Winnick W (1993) Langmuir 9:1319
14. Lin F, Meier DJ (1996) Langmuir 12:2774
15. Dhinojwala A, Torkelson JM (1994) Macromolecules 27:4817
16. Liu YS, Feng J, Winnik MA (1994) J Chem Phys 101:9096
17. Farinha JPS, Martinho JMG, Kawaguchi S, Yekta A, Winnik MA (1996) J Chem Phys 100:12552
18. Hahn K, Ley G, Schuller H, Oberthur R (1988) Colloid Polym Sci 266:631
19. Chevalier Y, Pichot C, Graillat C, Joanicot M, Wong K, Lindner P, Cabane B (1992) Colloid Polym Sci 270:806
20. Joanicot M, Wong K, Cabane B (1996) Macromolecules 29:4976
21. Sperry PR, Snyder BS, O'Dowd ML, Lesko PM (1994) Langmuir 10:2619
22. Ferry JD (1980) Viscoelastic Properties of Polymers, 3rd edn. Wiley, New York